

# A Disease-Associated MicroRNA Cluster Links Inflammatory Pathways and an Altered Composition of Leukocyte Subsets to Noninfectious Uveitis

Fleurieke H. Verhagen,<sup>1-3</sup> Cornelis P. J. Bekker,<sup>3</sup> Marzia Rossato,<sup>3</sup> Sanne Hiddingh,<sup>1,3</sup> Lieuwe de Vries,<sup>4</sup> Abhinandan Devaprasad,<sup>3</sup> Aridaman Pandit,<sup>3</sup> Jeannette Ossewaarde-van Norel,<sup>2</sup> Ninette ten Dam,<sup>2</sup> Maartje C. A. Moret-Pot,<sup>2</sup> Saskia M. Imhof,<sup>2</sup> Joke H. de Boer,<sup>1,2</sup> Timothy R. D. J. Radstake,<sup>1,3,5</sup> and Jonas J. W. Kuiper<sup>1-3</sup>

<sup>1</sup>Ophthalmology Unit, University Medical Center Utrecht, Utrecht University, Utrecht, The Netherlands

<sup>2</sup>Department of Ophthalmology, University Medical Center Utrecht, Utrecht University, Utrecht, The Netherlands

<sup>3</sup>Laboratory of Translational Immunology, University Medical Center Utrecht, Utrecht University, Utrecht, The Netherlands

<sup>4</sup>Department of Ophthalmology, Radboud University Medical Center Nijmegen, Nijmegen, The Netherlands

<sup>5</sup>Department of Rheumatology & Clinical Immunology, University Medical Center Utrecht, Utrecht University, Utrecht, The Netherlands

Correspondence: Fleurieke H. Verhagen, Department of Ophthalmology, University Medical Center Utrecht, Room B03.2.30, Heidelberglaan 100, 3584 CX Utrecht, The Netherlands; F.H.Verhagen@umcutrecht.nl

TRDJR and JJWK contributed equally to the work presented here and should therefore be regarded as equivalent authors.

Submitted: December 14, 2017

Accepted: January 16, 2018

Citation: Verhagen FH, Bekker CPJ, Rossato M, et al. A disease-associated microRNA cluster links inflammatory pathways and an altered composition of leukocyte subsets to noninfectious uveitis. *Invest Ophthalmol Vis Sci*. 2018;59:878-888. <https://doi.org/10.1167/iops.17-23643>

**PURPOSE.** The cause of noninfectious uveitis (NIU) is poorly understood but is considered to be mediated by a complex interplay between genetic, environmental, and—relatively unexplored—epigenetic factors. MicroRNAs (miRNAs) are noncoding small RNAs that are important epigenetic regulators implicated in pathologic signaling. Therefore, we mapped the circulating miRNA-ome of NIU patients and studied miRNA perturbations within the broader context of the immune system.

**METHODS.** We designed a strategy to robustly identify changes in the miRNA profiles of two independent cohorts totaling 54 untreated patients with active and eye-restricted disease and 26 age-matched controls. High-resolution miRNA-ome data were obtained by TaqMan OpenArray technology and subsequent RT-qPCR. Flow cytometry data, and proteomic data spanning the cellular immune system, were used to map the uveitis-miRNA signature to changes in the composition of specific leukocyte subsets in blood.

**RESULTS.** Using stringent selection criteria, we identified and independently validated an miRNA cluster that is associated with NIU. Pathway enrichment analysis for genes targeted by this cluster revealed significant enrichment for the PI3K/Akt, MAPK, FOXO, and VEGF signaling pathways, and photoreceptor development. In addition, unsupervised multidomain analyses linked the presence of the uveitis-associated miRNA cluster to a different composition of leukocyte subsets, more specifically, CD16<sup>+</sup>CD11c<sup>+</sup>HLA-DR<sup>-</sup> cells.

**CONCLUSIONS.** Together, this study identified a unique miRNA cluster associated with NIU that was related to changes in leukocyte subsets demonstrating systemic changes in epigenetic regulation underlying NIU.

**Keywords:** microRNA, uveitis, epigenetics, Birdshot, intraocular inflammation

Noninfectious uveitis (NIU) comprises a heterogeneous group of recurrent or chronic sight-threatening intraocular inflammations that eventually lead to permanent visual impairment or blindness in up to 19% of patients.<sup>1-4</sup> Since NIU affects more than 1 of every 1000 individuals and usually demands treatment for decades, the clinical and economic impact of NIU is enormous.<sup>5-7</sup>

NIU is well acknowledged as an immune-mediated disease. This is based upon (genetic) association with numerous immune-related molecules, the frequent occurrence of uveitis in relation to systemic inflammatory conditions, and the beneficial response to immunosuppressive therapy.<sup>8-12</sup> Despite our growing understanding that susceptibility to NIU is in part genetic, and epigenetic modulation contributes to various

ocular conditions, studies investigating the epigenetic landscape of uveitis are scarce.<sup>13-15</sup>

One of the mechanisms through which epigenetic regulation of gene expression takes place is through microRNAs (miRNAs).<sup>16</sup> miRNAs are small RNAs abundantly found in almost all biological tissues. miRNAs interfere with the translation of messenger RNA (mRNA) of more than half of the protein-coding genome and consequently orchestrate complex biological circuits including immunity.<sup>17-20</sup> Although miRNA binding to mRNA generally has a modest effect on protein expression, changes in the expression of miRNAs can have dramatic and widespread impact on cellular signaling.<sup>21</sup> As a result, a large number of profiling studies have been conducted to find changes in the levels of miRNAs that could potentially be used to diagnose or monitor disease or provide



novel therapeutic targets for treatment.<sup>22,23</sup> But despite their potential, miRNA profiling studies are particularly prone to low reproducibility and have hitherto delivered little clinical utility.<sup>24,25</sup> This can in part be attributed to experimental design (e.g., validation via independent cohorts). In addition, functional understanding of the implications of changes in miRNA levels is usually confined to knockdown and/or overexpression studies of only one or a few targets in single (nonprimary) cell types.<sup>26,27</sup>

To overcome the aforementioned limitations, we designed a strategy to robustly identify differences in the miRNA profile of the serum of patients with NIU.

## MATERIALS AND METHODS

### Patients and Patient Material

We collected blood from a total of 54 adult patients with one of three archetypical types of NIU: HLA-B27-associated acute anterior uveitis (AU), idiopathic intermediate uveitis (IU), or Birdshot uveitis (BU). Patients were seen at the outbound patient clinic of the Department of Ophthalmology of the University Medical Center Utrecht between July 2014 and December 2016. Patients were divided between a discovery cohort (AU:  $n = 9$ , IU:  $n = 9$ , BU:  $n = 10$ ) and a replication cohort (AU:  $n = 10$ , IU:  $n = 6$ , BU:  $n = 10$ ). All patients had active uveitis (new onset or relapse) at the time of sampling. None of the patients had a related systemic autoinflammatory or autoimmune disease, nor did they receive systemic immunomodulatory treatment in the last 3 months, other than a low dose of oral prednisolone ( $\leq 10$  mg,  $n = 1$ ).

Uveitis was classified and graded in accordance with the Standardization of Uveitis Nomenclature (SUN) classification.<sup>28</sup> For detailed information on the clinical workup see Supplementary Methods. Twenty-six age- and sex-matched anonymous blood donors with no history of ocular inflammatory disease (UMC Utrecht) served as unaffected controls.

This study was conducted in compliance with the Declaration of Helsinki. Ethical approval was requested and obtained from the Medical Ethical Research Committee in Utrecht and all patients signed written informed consent before participation.

### MicroRNA Profiling: OpenArray

Total RNA was extracted from 200  $\mu$ L serum by using Exiqon's miRCURY RNA Isolation Kit for biofluids (Exiqon, Vedbaek, Denmark), according to the manufacturer's instructions. RNA extraction was performed for all serum samples on the same day and the order of samples randomized according to previous recommendations.<sup>29</sup> Because there are currently no universally applicable endogenous serum control miRNAs and to facilitate reproducibility (standardized controls), we used nonhuman miRNA (ath-miR-159a) as a spike-in control for normalization.<sup>30</sup> More details on RNA isolation are provided in the Supplementary Methods.

We screened for 758 miRNAs in the serum of the discovery cohort by using the TaqMan OpenArray platform (Thermo Fisher, Waltham, MA, USA) according to the manufacturer's instructions (see also Supplementary Methods). The resulting expression levels, given in cycle threshold (Crt) values of all miRNAs, were normalized by subtraction of the mean Crt value of the spike-in, resulting in a deltaCrt ( $\Delta\text{Crt} = \text{Crt}_{\text{mean target}} - \text{Crt}_{\text{mean miR-159a}}$ ). Differences in miRNA expression levels between patients and controls were assessed by comparing these  $\Delta\text{Crt}$  values of patients to healthy controls, using the comparative threshold cycle method.<sup>31</sup> In short, expression

levels are presented as the fold change ( $\text{FC} = 2^{-\Delta\Delta\text{Ct}}$ , where  $\Delta\Delta\text{Crt} = \Delta\text{Crt}_{\text{patient}} - \Delta\text{Crt}_{\text{reference}}$ ) as compared to the healthy control that represented the median of the spike-in and was set to 1 (FC). miRNAs were selected for validation if they were well expressed (mean Crt  $< 27$ , amplification score of  $> 1.24$ ), in  $> 90\%$  of all samples, with FC of  $\geq 2$  or  $< 0.5$ , and a  $P$  value of  $< 0.05$ .

### Validation of miRNAs: TaqMan Single RT-qPCR

We performed TaqMan single quantitative reverse transcription-PCR (RT-qPCR) (see also Supplementary Methods) for 10 miRNAs that passed the selection criteria, on the same samples from the discovery cohort. The Ct values from the TaqMan assay were compared with the Crt values from the OpenArray platform. miRNAs were considered technically validated when Spearman's  $\rho > 0.5$  and  $P < 0.05$ . All validated miRNAs were tested in a second, independent replication cohort ( $n = 36$ ) for biological validation.

### Statistical Approaches

The OpenArray output was analyzed by using the Thermo Fisher Cloud software, which follows an independent samples  $t$ -test to compare  $\Delta\Delta\text{C}(r)t$  data with a  $P$  value threshold below 0.05 (two-tailed). To facilitate discovery of potentially meaningful mediators, we applied correction for multiple testing only to the combined data set (discovery + replication strategy), which was obtained after a more robust three-staged cohort of discovery, validation, and replication using independent technologies and cohorts. In the combined cohorts, nonparametric tests (Mann-Whitney  $U$  test, Kruskal-Wallis with post hoc Dunn's with adjusted  $P$  values, Spearman's  $\rho$ ) were used to compare groups or test for correlations. Selected individual miRNAs were subjected to receiver operating characteristic (ROC) curves using the FC values.

Details on the association between miRNAs ( $\Delta\Delta\text{Ct}$ ) and clinical characteristics are described in Supplementary Methods. To correct for multiple testing, a  $P$  value of  $< 0.0055$  (0.05/9 clinical parameters) was considered significant.

The FC values (or singular value decomposition imputed values, max 10%) for miRNAs that met the amplification and expression criteria were subjected to unsupervised hierarchical clustering (Euclidian distance, Ward's linkage method). Clustering was performed with ClustVis or MetaboAnalyst.<sup>32,33</sup> Statistical analyses were performed in SPSS version 21.0 (SPSS, Inc., Chicago, IL, USA), GraphPad Prism (GraphPad, La Jolla, CA, USA), MetaboAnalyst Server v3.0, and R v3.3.2.

### Target Analysis

Predicted and reported mRNA targets of the validated miRNAs were mapped by using miRGATE<sup>34</sup> and MirTargetLink.<sup>35</sup> Pathway enrichment analysis was performed for Gene Ontology (GO) biological processes,<sup>36</sup> Kyoto Encyclopedia of Genes and Genomes (KEGG) pathways,<sup>37</sup> and Pathway Ontology (PW) pathways<sup>38</sup> on all gene targets that were targeted by at least two miRNAs, using ToppGene Suite (BMI CCHMC, Cincinnati, OH, USA).<sup>39</sup> To visualize shared pathways, unsealed false discovery rate (FDR)-corrected  $P$  values for pathways related to inflammation and eye biology were outlined in a heatmap generated by Clustvis software.<sup>32</sup>

### Leukocyte Cell Subset MicroRNA and Proteome Analyses

Global miRNA expression data for nine primary leukocyte populations were derived from four noncoding RNA micro-

TABLE. Characteristics of the Discovery and Replication Cohorts Investigated in This Study

	AU	IU	BU	HC	P Value
Discovery Cohort					
N	9	9	10	16	N/A
Male/female	3/6	2/7	4/6	6/10	0.90*
Age, mean ± SD, y	47.7 ± 17.0	39.3 ± 14.0	52.9 ± 13.2	41.4 ± 9.8	0.09**
Disease duration, median (range), y	5.8 (0.1–39.3)	3.7 (0.2–20.0)	1.3 (0.2–15.1)	N/A	0.14***
Replication Cohort					
N	10	6	10	10	N/A
Male/female	2/8	3/3	6/4	4/6	0.39*
Age, mean ± SD, y	45.9 ± 16.1	31.7 ± 10.5	45.8 ± 12.2	41.5 ± 14.0	0.19**
Disease duration, median (range), y	8.1 (0.2–22.3)	4.9 (0.4–14.1)	0.9 (0.2–33.2)	N/A	0.41***

AU, HLA-B27-associated anterior uveitis; HC, healthy control; N/A, not applicable.

\* Fisher's exact test.

\*\* ANOVA.

\*\*\* Kruskal-Wallis.

array data sets available via the Gene Expression Omnibus (see Supplementary Methods). Normalized miRNA profiles ( $n = 825$ ) for these leukocyte subsets were subjected to hierarchical clustering or principle component analysis to interrogate global miRNA expression profiles (MetaboAnalyst 3.0).<sup>35</sup> Mass spectrometry-based proteomics data for the nine primary leukocyte subsets (162 samples) were used to obtain the cell-specific protein expression data.<sup>40</sup> For detailed information see Supplementary Methods.

### Flow Cytometry Analysis of Lymphoid and Myeloid Populations

Peripheral blood mononuclear cells (PBMCs) from 30 patients and 15 healthy controls were obtained by Ficoll gradient centrifugation and stored at  $-80^{\circ}\text{C}$ . Thawed PBMCs were stained with antibodies listed in Supplementary Table S1, randomized for measurement by BD LSR Fortessa Cell Analyzer (BD Bioscience, San Jose, CA, USA). Samples were grouped according to low miR-233-3p versus high miR-233-3p levels (cutoff  $< \text{FC } 1.29 \geq$  median of unaffected controls; Supplementary Table S2).

To minimize technical variability inherent to manual gating, we performed unsupervised hierarchical clustering by using Citrus<sup>41</sup> on 50,000 random events from pre-gated (Supplementary Fig. S1) viable single cells exported from Flow Jo Software for each sample with a 1% minimum cluster size to reduce granularity and arcsin hyperbolic transformation value at 200. In short, Citrus applies an unsupervised clustering algorithm to map the hierarchy of phenotypically related cell clusters, which results in a so-called tree. This is followed by a supervised classification model to highlight stratifying clusters for predefined conditions (high versus low miRNA levels). Cells were clustered by the expression of lineage (CD3/CD56/CD19), CD14, CD1c, HLA-DR, CD123, CD11c, CD141, and CD303 proteins. Since we investigated groups with unequal numbers of samples, we explored the abundance of cell populations by using the significance analysis of microarrays (SAM) with significance inferred for false discovery rate  $< 1\%$ .

## RESULTS

### High-Throughput miRNA Profiling Reveals 10 Differentially Expressed miRNAs

We devised a three-staged strategy with stringent selection criteria to identify differently expressed miRNAs in serum of NIU patients (Supplementary Fig. S2). The demographic data of

the NIU patients and controls from the discovery cohort and the replication cohort are shown in the Table. First, we screened for 758 circulating miRNAs in 28 patients and 16 healthy controls (discovery cohort) by using a high-throughput real-time PCR platform (OpenArray). A total of 102 miRNAs passed quality control (Supplementary Table S3). We could distinguish patients from controls from the overall miRNA profile (Fig. 1), which exhibited mostly increased levels for most detected miRNAs (Supplementary Fig. S3). To aid in the elimination of background variation and improve reproducibility of our findings, we maintained a stringent 2-fold change cutoff and  $P < 0.05$  for significance. This approach yielded six miRNAs (miR-140-5p, miR-491-5p, miR-223-3p, miR-223-5p, miR-193a-5p, and miR-29a-3p) and a small nuclear RNA (U6 snRNA) that were upregulated in one or more patient groups compared to healthy controls (Supplementary Fig. S3; Supplementary Table S4). Between the uveitis groups, three miRNAs (miR-127-3p, miR-375, miR-409-3p) were differentially expressed (Supplementary Fig. S3; Supplementary Table S4), resulting in a total of 10 miRNAs that were selected for replication.

High-throughput miRNA profiling technologies are inherently prone to detect certain miRNAs over others.<sup>42,43</sup> We performed several investigations that showed no apparent detection bias and thus we consider the detected miRNA profile a genuine representative sample of the blood-borne miRNA-ome of NIU (see Supplementary Methods; Supplementary Fig. S4).

### Replication of Seven Serum miRNAs in an Independent Cohort

We next technically validated the miRNAs from the discovery cohort by using RT-qPCR. The expression levels for 9/10 miRNAs demonstrated strong correlation ( $\rho$ , 0.55–0.97; all  $P \leq 0.0001$ ) between these technologies and were thus considered technically validated (Fig. 2; Supplementary Table S4). Next, we investigated the levels of these nine miRNAs in an independent cohort of 26 patients and 10 controls (Table). Biological replication was achieved for six miRNAs (miR-140-5p, miR-193a-5p, miR-223-3p, miR-223-5p, miR-29a-3p, and miR-491-5p) and U6 snRNA in at least one of the uveitis disease groups versus healthy controls (Fig. 2; Supplementary Table S4). All were significantly more highly expressed in uveitis patients than the controls (Fig. 2D).

Since an increase in the levels of the replicated miRNAs was observed for all uveitis subtypes, we combined the TaqMan RT-qPCR data from both cohorts to investigate the discriminative power of the uveitis-associated cluster. The analysis of the area



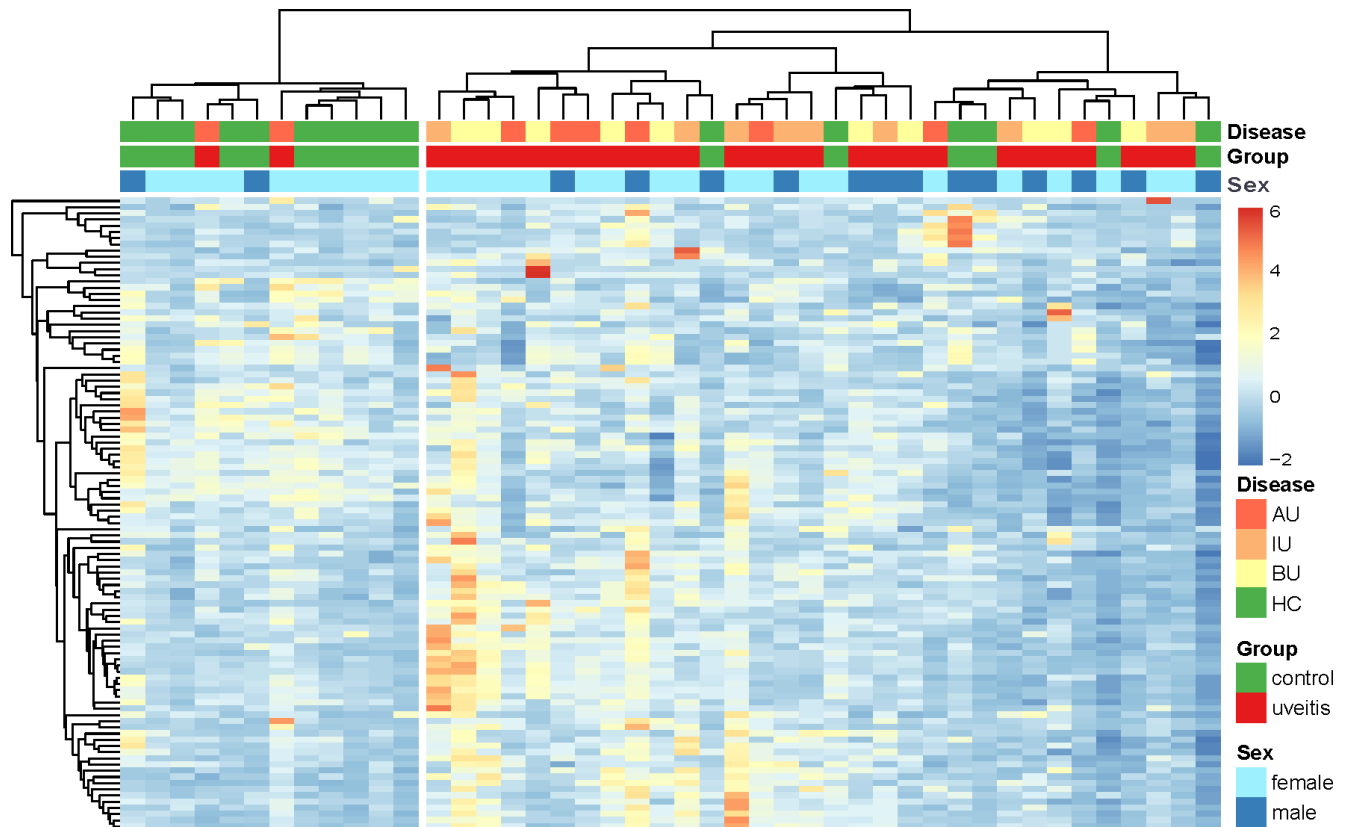


**FIGURE 1.** Unsupervised hierarchical clustering of the serum miRNA-ome of the discovery cohort. Heatmap of unsupervised hierarchical clustering based on 102 detected miRNAs that met quality control thresholds from the discovery cohort (screening study). Depicted are the transformed FC values (see Materials and Methods) from patients with HLA-B27-associated uveitis (AU), IU, BU, and healthy controls (HCs). Unit variance scaling is applied to rows. Heatmap colors represent the fold changes in a color-coded way: *blue* (low) to *red* (high). Clustering was performed with ClustVis using correlation distance and Ward linkage and is depicted as dendrograms for columns and rows.

under the ROC curve revealed that these miRNAs displayed relatively good specificity and sensitivity (Supplementary Table S2).

We observed no statistically significant correlations between the levels of selected miRNAs and age, sex, lymphocyte and leukocyte count, development of ocular complications, or need for treatment with systemic medication. Interestingly, we did find an inverse correlation between disease duration and the serum levels of U6 snRNA, which was seemingly driven by AU patients (Supplementary Fig. S5).

### Uveitis-Associated miRNA Cluster Targets Inflammatory and Ocular Biology Pathways

To aid in the understanding of the widespread downstream effects of the identified miRNAs in NIU, we narrowed down relevant disease pathways by selecting genes targeted by at least two of the uveitis-associated miRNAs by using miRTargetLink.<sup>35</sup> Together, six miRNAs shared 37 gene targets (Fig. 3A). Pathway enrichment analysis (see Materials and Methods) for these overlapping gene targets revealed significant (FDR-corrected  $P < 0.05$ ) enrichment for inflammatory and ocular biology pathways (Fig. 3B).

### The NIU-Specific miRNA Cluster Is Associated With Altered Frequencies of CD16<sup>+</sup> Leukocytes

The expression levels of the seven miRNAs were strongly correlated with each other and therefore further considered as

a single uveitis-associated miRNA cluster (Fig. 3C; Supplementary Fig. S6). We hypothesized that the uveitis-associated miRNA cluster can reflect specific changes in leukocyte populations.<sup>44–47</sup> To investigate this, we first used noncoding RNA array data (825 overlapping miRNAs) across 113 samples of nine primary leukocyte populations—covering most cell populations of the immune system. Consistent with literature, the derived miRNA-ome was highly cell-type specific (Fig. 4A). Principle component analysis clearly distinguished a lymphoid cluster (T cells, B cells, natural killer [NK] cells) and two myeloid clusters (Fig. 4B). Among the major miRNAs contributing to the clustering of these populations were miR-223-3p and miR-29a-3p (Fig. 4B; Supplementary Fig. S7). The expression of the other uveitis-associated miRNAs also varied considerably between the populations (Supplementary Fig. S8). Using correlation, we mapped the uveitis-associated miRNAs to remote clusters of expression across the leukocyte populations (Supplementary Fig. S9). To verify whether the distinguished expression of the miR-29a-3p and miR-223-3p across the leukocyte subsets reflects meaningful downstream biological differences, we mined mass spectrometry-based proteomic data of the investigated cell subsets ( $n = 162$ ) for the expression of validated target genes (Supplementary Fig. S10; Supplementary Table S5). Unsupervised hierarchical clustering of the miRNA-target proteome of miR-29a-3p and miR-223-3p clearly discerned the myeloid and lymphoid cell subsets (Fig. 4C).

Finally, we wished to explore whether the miRNA cluster tagged changes in specific leukocyte subsets in uveitis patients.

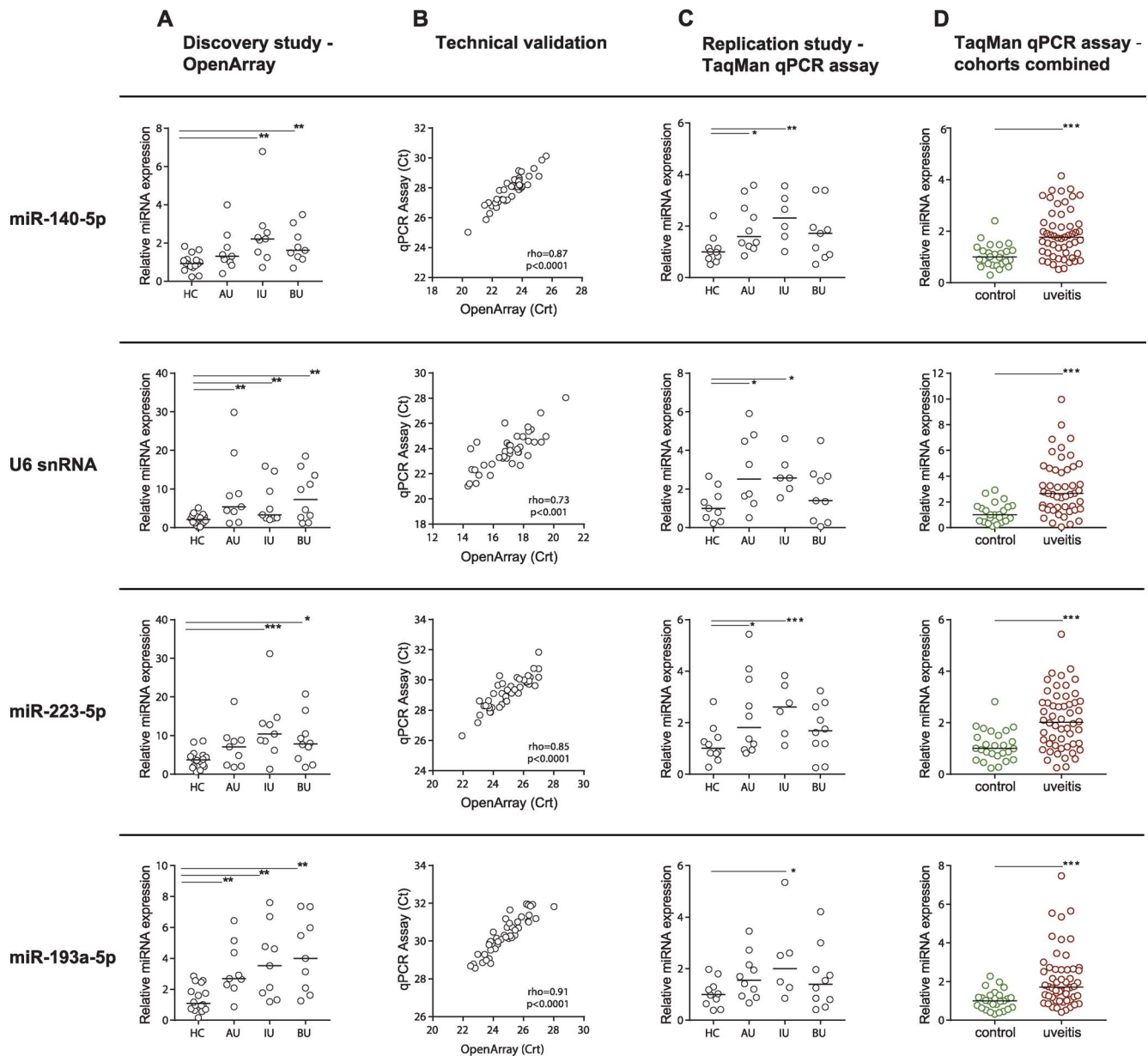


**FIGURE 2.** Discovery, validation, and replication of seven miRNAs increased in serum of patients with noninfectious uveitis. From *left to right*: (A) Results from OpenArray in discovery cohort ( $n = 44$ ). On the  $y$ -axis are the relative expression levels (i.e., the transformed FC values [see Materials and Methods]) shown for the patients as compared to the mean expression of healthy controls.  $P$  values are from independent  $t$ -test. (B) Correlation between expression levels for selected miRNAs obtained by OpenArray and TaqMan single RT-qPCR assay. Spearman's  $\rho$  is used to test for correlation. (C) Results from TaqMan single RT-qPCR assay in the replication cohort ( $n = 36$ ). On the  $y$ -axis are the relative expression levels (i.e., the transformed FC values [see Materials and Methods]) shown for the patients as compared to the mean expression of healthy controls.  $P$  values are from independent samples  $t$ -test. (D) Results from TaqMan single RT-qPCR assay of both cohorts combined ( $n = 80$ ) and stratified for uveitis patients and healthy controls.  $P$  values are from Mann-Whitney  $U$  test (uveitis versus control). AU, HLA-B27-associated anterior uveitis; HC, healthy control. \* $P < 0.05$ , \*\* $P < 0.01$ , \*\*\* $P < 0.001$ , \*\*\*\* $P < 0.0001$ .

To this aim, we exploited available flow cytometry data from 30 NIU patients and 15 controls from this study (see Supplementary Methods; Supplementary Table S2). Unbiased computational mining of the flow cytometry data by Citrus identified two cell clusters that displayed significantly changed cell abundance according to the expression of the miRNA signature. These included a cluster of lymphocytes (cluster A; Figs. 4D, 4E, and Supplementary Fig. S11) and a cluster of populations characterized by high CD16 expression, dim expression of lineage marker (lin<sup>dim</sup>) and CD11c, and low levels of HLA-DR and the monocyte marker CD14 (cluster B1-3, Supplementary Fig. S11), reminiscent of CD16<sup>+</sup> CD56<sup>dim</sup> NK

cells.<sup>48</sup> This CD16<sup>+</sup> cluster also contained populations with low but distinguished expression of CD141 and CD303, most likely residual granulocyte populations (cluster B2 and B3; Figs. 4D, 4E).<sup>49,50</sup> These observations link a disease-associated circulating miRNA cluster with marked changes in the leukocyte repertoire in the blood of patients with NIU.

## DISCUSSION

Using a high dimensional and multilevel approach we identified and independently validated the presence of a

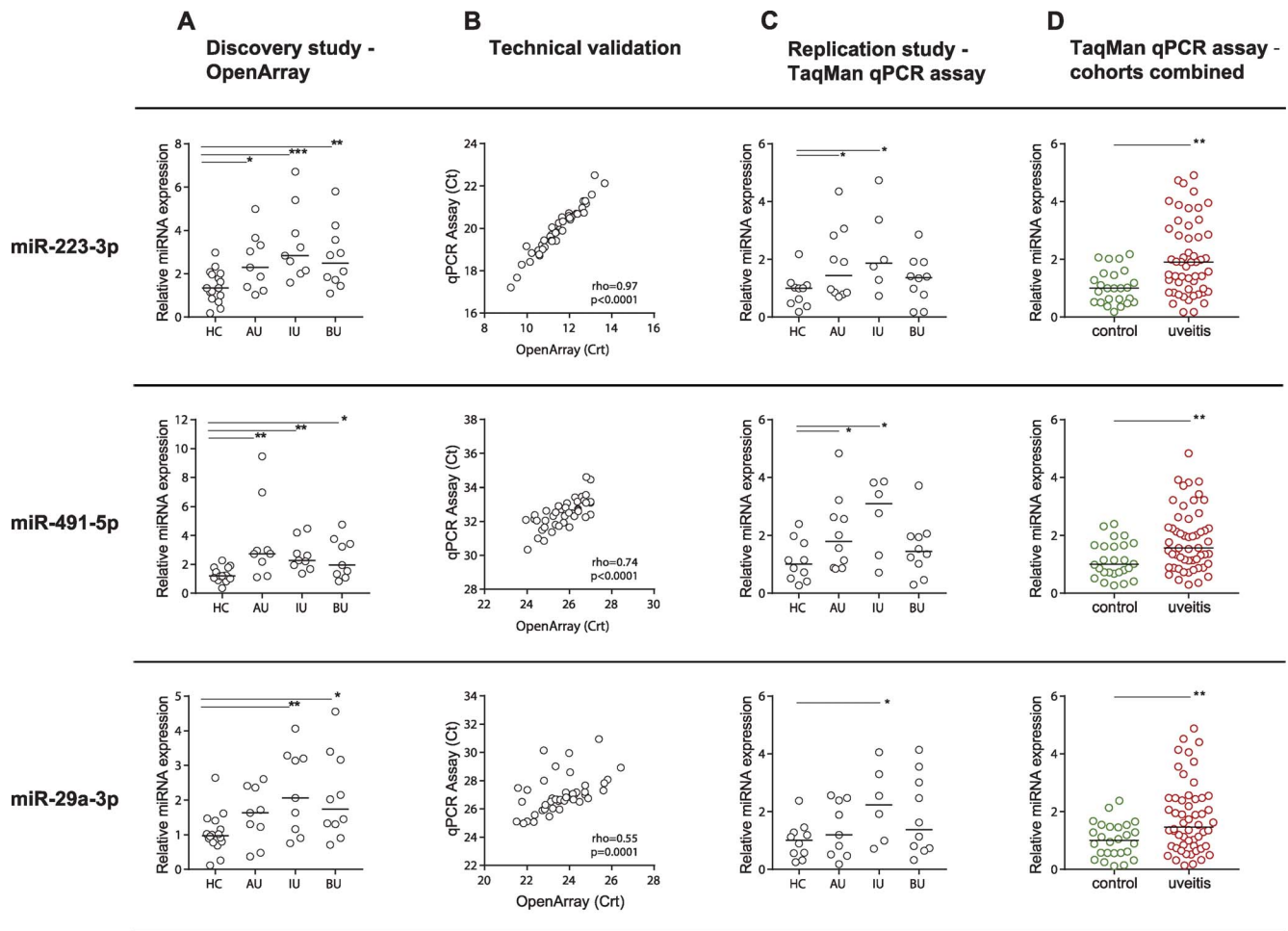


FIGURE 2. Continued

uveitis-specific miRNA cluster. This uveitis cluster comprised six miRNAs and a small nuclear RNA that suggest the involvement of several inflammatory signaling cascades (PI3K/Akt, MAPK, FOXO, and VEGF signaling) involved in several eye diseases. In addition, our work showed improved power to validate (70% of selected miRNAs were replicated) as well as to understand the potential role of circulating miRNAs in pathologic conditions without the necessity to have large cohorts.

NIU denotes a collective of clinically heterogeneous intraocular inflammatory diseases that share immune characteristics with—and commonly form an underappreciated feature of—systemic (auto)inflammatory conditions.<sup>10,51–53</sup> This led us to deliberately study two cohorts (discovery and replication cohort) of treatment-free patients with eye-restricted and active disease. This allowed us to better address the impact of intraocular inflammation on miRNAs in the circulation. To the best of our knowledge, this resulted in the first miRNA investigation of NIU patients without underlying (or potentially confounding) systemic disease.<sup>54–56</sup>

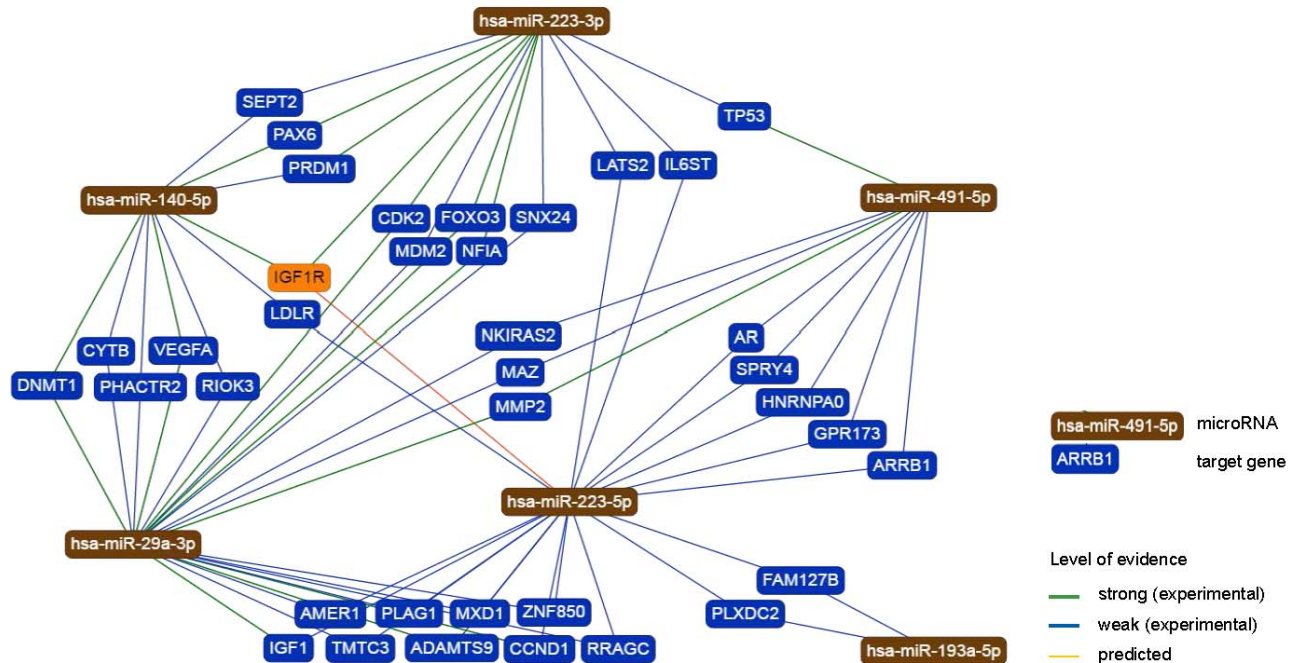
The main aim of the study was to explore the circulating miRNA profile of NIU to better understand its enigmatic etiology and lay the groundwork for emerging noncoding RNA-based therapeutics to reverse NIU.<sup>57</sup> Yet, a major obstacle for bringing small RNAs into consideration for therapeutic targeting is the notoriously low concordance and reproducibility between available technologies for detecting differential expression, which consequently results in conflicting reports

on candidate identification. Although recommendations for quality control<sup>58</sup> have improved reproducibility, we also invested additional efforts in assembling an independent replication cohort to be able to identify a robust set of uveitis-associated miRNAs.

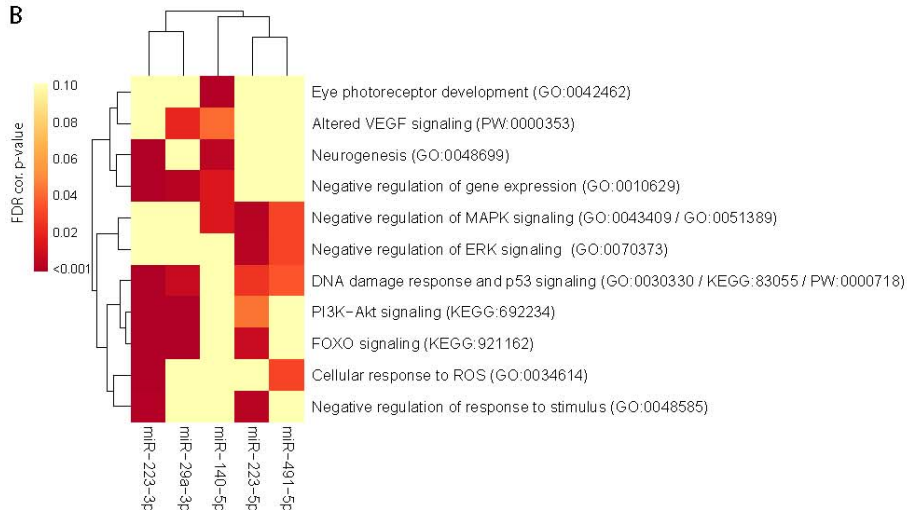
The quest for understanding the downstream effects of serum miRNA perturbations is a highly ambiguous one. Individual miRNAs regulate numerous genes, while a single gene can be regulated by a panel of miRNAs.<sup>17,59</sup> Yet, most biological processes are tuned by the concerted action of multiple miRNAs targeting the same pathways.<sup>18,19,60</sup> Given the close correlation of miRNA levels, as well as overlapping predicted and experimentally validated pathways, it is tempting to speculate that the identified miRNA signature acts as a pathologic ensemble driving—or responding to—ocular inflammation. Functional experiments with appropriate multi-miRNA knockout and conditional (over)expression models will be necessary to pinpoint the functional consequences of our observations.

Several recent key studies highlight the importance of our observations. miR-223-3p is upregulated in animal models of uveitis and is able to drive inflammation via T cells and myeloid dendritic cells, two cell types that are implicated in the biology of uveitis.<sup>10,61–65</sup> Myeloid-derived mir-223 is critical to innate immunity during gut inflammation, and skewed serum levels of this miRNA may hint toward a dysbiotic microbiome.<sup>66–68</sup> This is particularly interesting, since commensal microbiota can trigger autoimmune uveitis in mice.<sup>69</sup> Consequently, miR-223-

A



B



C

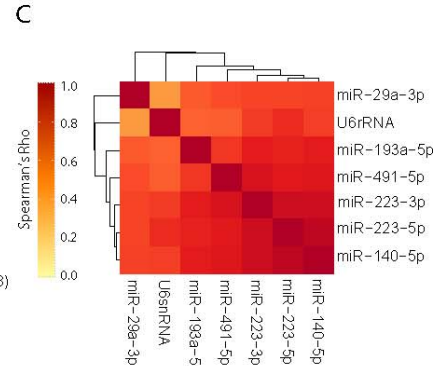


**FIGURE 3.** miRNA-target analysis of the validated serum microRNAs in noninfectious uveitis. (A) miRNA-target network of established overlapping mRNA targets of the uveitis-associated miRNAs. miRNAs are depicted in *brown boxes* and the mRNA targets are depicted in *blue* (targeted by two miRNAs) or *orange* (targeted by three miRNAs) boxes. Lines indicate level of evidence: strong (*green*), weak (*blue*), or predicted (*yellow*). Figure generated with MirTargetLink. (B) Heatmap of unscaled FDR-corrected *P* values for miRNA-target pathways related to inflammation and eye biology. Pathway analysis (ToppGene suite<sup>39</sup>) was performed on mRNA targets that were shared between at least two miRNAs. Clustering was performed by using Euclidean distance and Ward linkage. (C) Heatmap of unsupervised hierarchical clustering of the correlation of expression (TaqMan RT-qPCR for the discovery and replication cohorts combined) for validated serum cluster. Heatmap colors represent Spearman's  $\rho$  (calculated on ddCT). ERK, extracellular regulated kinase; FoxO, Forkhead box O; MAPK, mitogen-activated protein kinase; PI3K, phosphatidylinositol 3-kinase; ROS, reactive oxygen species; VEGF, vascular endothelial growth factor.

3p has been suggested as a good candidate for miRNA targeting in the treatment of inflammatory diseases such as NIU.<sup>70</sup>

We explored if the levels of the uveitis-associated signature were correlated with changes in specific blood cell populations of these same patients. We focused on leukocytes because previous studies have highlighted a predominant function of leukocytes in uveitis.<sup>10</sup> We realize that the flow

cytometry panels used here may lack the resolution needed for an in-depth analysis of all leukocyte populations in blood (outside the scope of this study), yet we were able to highlight several interesting changes; we identified a decreased frequency of a cell population distinguished by high CD16 expression. As based on other cell surface makers (CD11c<sup>+</sup>HLA-DR<sup>+</sup>CD14<sup>+</sup>lin<sup>dim</sup>), this cluster most likely represents the



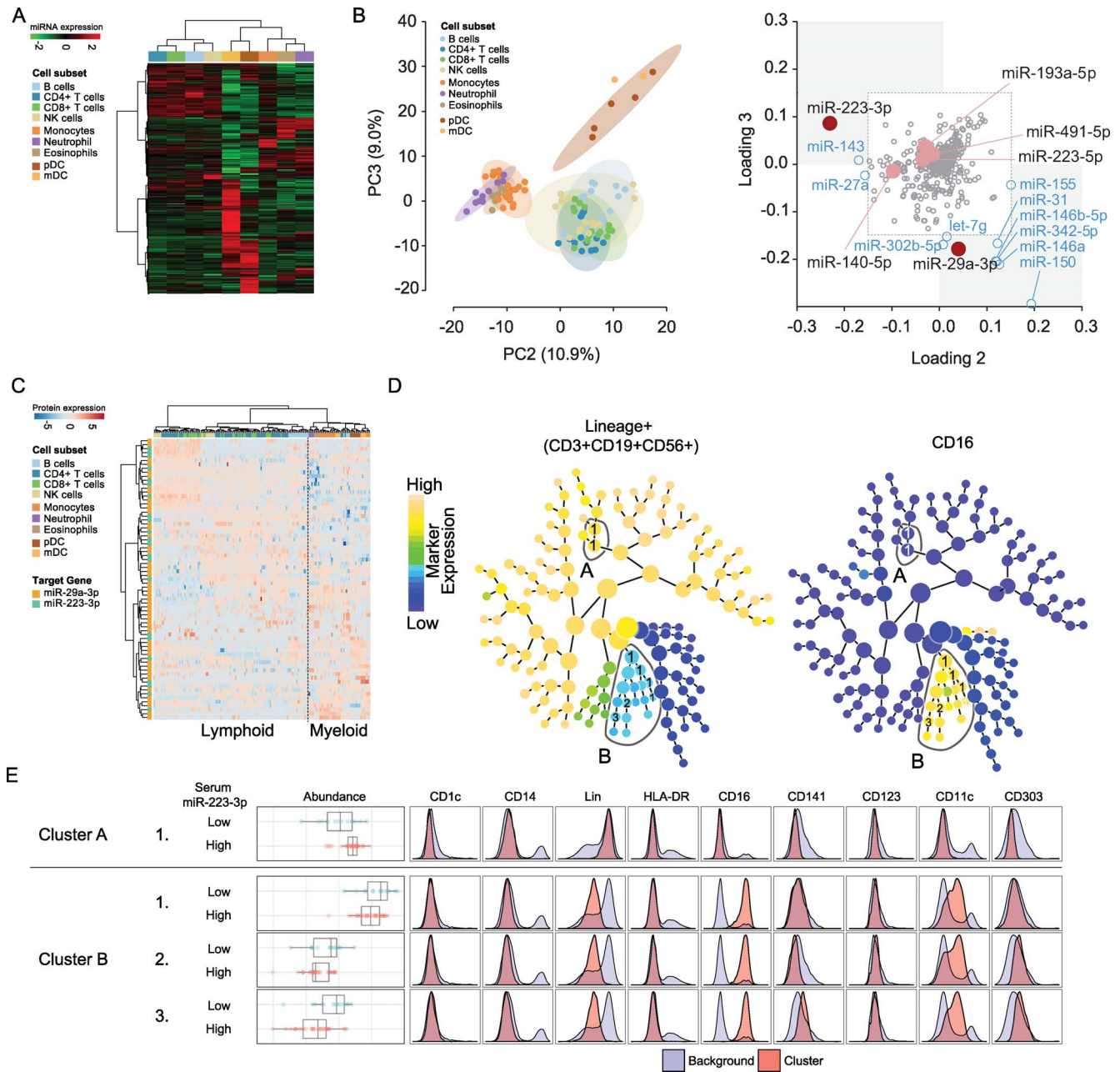


**FIGURE 4.** Meta-analysis of the leukocyte miRNA-ome links the uveitis-associated cluster to leukocyte composition in blood. **(A)** Meta-analysis of the cellular miRNA-ome ( $n = 825$ ) of nine primary leukocyte populations ( $n = 113$ ). Indicated is the average relative cellular miRNA expression for each investigated cell subset. Ward's method of hierarchical clustering of miRNA data was performed with Pearson correlation distance. **(B)** Principle component analysis (PCA) of the cellular miRNA-ome of the leukocyte subsets. Three populations are clearly distinguishable by the second and third principal components. Loading plot of PCA shows that miR-29a-3p and miR-223-3p (dark red) are among the top miRNAs (>1.5 loading score, light blue) that contribute to these clusters. The relative position of the other uveitis-associated miRNAs is indicated. **(C)** Unsupervised hierarchical clustering of proteomic data of validated target genes ( $n = 74$ ; Supplementary Fig. S9, Supplementary Table S4) for miR-29a-3p and miR-223-3p in nine leukocyte cell subsets (see Materials and Methods) distinguishes lymphocyte and myeloid populations. **(D)** Citrus tree of identified common cell populations (>1% of sample) in blood that distinguishes individuals with relatively high levels of the uveitis-associated miRNA cluster from individuals with relatively lower levels in serum. Contours indicate clusters (A and B) with a significantly different abundance in individuals with relatively higher miRNA levels (SAM, by FDR of 1%). Expression of CD16 and lineage (CD3/CD19/CD56) marker is indicated in color scale. High-dimensional phenotype for each cluster is outlined in Supplementary Figure S10. **(E)** Histogram plots of the relative expression of each cell surface marker by the identified clusters (red) compared to the overall expression of all other clusters (blue). The relative abundance of the identified clusters in individuals with high/low levels of the uveitis-associated miRNA cluster is indicated.

cytotoxic CD16<sup>+</sup>CD56<sup>dim</sup> NK cells, a cell type that plays a critical role in the first line of defense against infected, cancerous, and autoreactive cells. Also, this is the major NK subset in blood that typically expresses killer immunoglobulin-

like receptors, a receptor that is implicated in the biology of NIU.<sup>48,71</sup>

It is tempting to speculate that the increased frequency of the lymphocyte cluster represents CD4<sup>+</sup> T cells. We observed



that the uveitis-associated miR-140-5p and miR-29a-3p are typically more highly expressed in lymphocyte populations, including CD4<sup>+</sup> T cells. miR-140-5p, which had the highest discriminative power between uveitis patients and controls, is aberrantly expressed and implicated in pathogenic T-cell function in multiple sclerosis,<sup>72,73</sup> a disease linked to IU.<sup>74-76</sup> It is important to emphasize, however, that the functions of miR-140-5p (and miR-29a-3p) most likely expand beyond T-cell function. For example, we also noted associated pathways relevant for ocular biology, including VEGF signaling,<sup>77-79</sup> photoreceptor development, and retina homeostasis.<sup>80,81</sup> These ocular biology pathways may attempt to control damage to ocular tissues.

U6 snRNA is a small nuclear RNA (snRNA) that is normally localized in the nucleus, but blood microvesicles or exosomes—which vastly increase in number in the circulation during inflammation<sup>82</sup>—are also particularly enriched for U6 nuclear RNA.<sup>83,84</sup> Curiously, U6 snRNA is widely used for normalization of miRNA expression studies,<sup>85,86</sup> while we here showed that the levels of this miRNA are robustly upregulated in the serum of uveitis patients. This is also increasingly reported for other conditions.<sup>87-90</sup>

Our results have to be interpreted with the following study limitations in mind. First, although we believe that our stringent selection criteria contributed to the robust identification and replication of uveitis-associated miRNAs, it consequently also limited sample size and power to detect more subtle differences. It seems reasonable to speculate that this may have prevented the detection of a relation between the miRNA levels and heterogeneous clinical end-points, and hampered the validation of differences between uveitis subtypes. Overall, we would like to emphasize that the study of miRNAs in serum is by no means exhaustive, and recapitulate that the identified miRNAs most likely function in clusters of functionally related mediators that orchestrate molecular route function into complex behavior of the immune system in uveitis. As such, the here identified miRNA signature serves as an important starting point to further functionally dissect the epigenetic regulation by these miRNAs and their interaction within the cellular immune system of patients with NIU.

In conclusion, our data demonstrate systemic changes in epigenetic regulation that link serum miRNA levels to changes in leukocyte populations underlying inflammatory eye disease.

### Acknowledgments

The authors thank Eleni Chouri and Jorre Mertens for analytical support and useful discussions.

Supported by unrestricted grants from Dr. F.P. Fischer-Stichting and LSBS. The funders had no role in study design, data collection and analysis, decision to publish, or preparation of the manuscript.

Disclosure: **F.H. Verhagen**, None; **C.P.J. Bekker**, None; **M. Rossato**, None; **S. Hiddingh**, None; **L. de Vries**, None; **A. Devaprasad**, None; **A. Pandit**, None; **J. Ossewaarde-van Norel**, None; **N. ten Dam**, None; **M.C.A. Moret-Pot**, None; **S.M. Imhof**, None; **J.H. de Boer**, None; **T.R.D.J. Radstake**, None; **J.J.W. Kuiper**, None

### References

- Durrani OM, Tehrani NN, Marr JE, Moradi P, Stavrou P, Murray PI. Degree, duration, and causes of visual loss in uveitis. *Br J Ophthalmol*. 2004;88:1159-1162.
- Dick AD, Tundia N, Sorg R, et al. Risk of ocular complications in patients with noninfectious intermediate uveitis, posterior uveitis, or panuveitis. *Ophthalmology*. 2016;123:655-662.
- Verhagen FH, Brouwer AH, Kuiper JJW, Ossewaarde-van Norel J, ten Dam-van Loon NH, de Boer JH. Potential predictors of poor visual outcome in human leukocyte antigen-B27-associated uveitis. *Am J Ophthalmol*. 2016;165:179-187.
- Tomkins-Netzer O, Talat L, Bar A, et al. Long-term clinical outcome and causes of vision loss in patients with uveitis. *Ophthalmology*. 2014;121:2387-2392.
- Thorne JE, Suhler E, Skup M, et al. Prevalence of noninfectious uveitis in the United States. *JAMA Ophthalmol*. 2016;134:1237-1245.
- Muñoz-Fernández S, Martín-Mola E. Uveitis. *Best Pract Res Clin Rheumatol*. 2006;20:487-505.
- De Smet MD, Taylor SRJ, Bodaghi B, et al. Understanding uveitis: the impact of research on visual outcomes. *Prog Retin Eye Res*. 2011;30:452-470.
- Perez VL, Caspi RR. Immune mechanisms in inflammatory and degenerative eye disease. *Trends Immunol*. 2015;36:354-363.
- Yang M-M, Lai TYY, Luk FOJ, Pang C-P. The roles of genetic factors in uveitis and their clinical significance. *Retina*. 2014;34:1-11.
- Lee RW, Nicholson LB, Sen HN, et al. Autoimmune and autoinflammatory mechanisms in uveitis. *Semin Immunopathol*. 2014;36:581-594.
- Hou S, Kijlstra A, Yang P. Molecular genetic advances in uveitis. *Prog Mol Biol Transl Sci*. 2015;134:283-298.
- Kuiper J, Rothova A, de Boer J, Radstake T. The immunopathogenesis of birdshot chorioretinopathy: a bird of many feathers. *Prog Retin Eye Res*. 2015;44:99-110.
- Liu MM, Chan C-C, Tuo J. Epigenetics in ocular diseases. *Curr Genomics*. 2013;14:166-172.
- Berber P, Grassmann F, Kiel C, Weber BHF. An eye on age-related macular degeneration: the role of microRNAs in disease pathology. *Mol Diagn Ther*. 2017;21:31-43.
- Pradhan P, Upadhyay N, Tiwari A, Singh LP. Genetic and epigenetic modifications in the pathogenesis of diabetic retinopathy: a molecular link to regulate gene expression. *New Front Ophthalmol*. 2016;2:192-204.
- Dawson MA, Kouzarides T. Cancer epigenetics: from mechanism to therapy. *Cell*. 2012;150:12-27.
- Iwakawa HO, Tomari Y. The functions of microRNAs: mRNA decay and translational repression. *Trends Cell Biol*. 2015;25:651-665.
- Londin E, Loher P, Telonis AG, et al. Analysis of 13 cell types reveals evidence for the expression of numerous novel primate- and tissue-specific microRNAs. *Proc Natl Acad Sci U S A*. 2015;112:E1106-E1115.
- Kozomara A, Griffiths-Jones S. miRBase: integrating microRNA annotation and deep-sequencing data. *Nucleic Acids Res*. 2011;39:D152-D157.
- Lewis BP, Burge CB, Bartel DP. Conserved seed pairing, often flanked by adenosines, indicates that thousands of human genes are microRNA targets. *Cell*. 2005;120:15-20.
- Baek D, Villén J, Shin C, Camargo FD, Gygi SP, Bartel DP. The impact of microRNAs on protein output. *Nature*. 2008;455:64-71.
- Schwarzenbach H, Nishida N, Calin GA, Pantel K. Clinical relevance of circulating cell-free microRNAs in cancer. *Nat Rev Clin Oncol*. 2014;11:145-156.
- Zeng L, Cui J, Wu H, Lu Q. The emerging role of circulating microRNAs as biomarkers in autoimmune diseases. *Autoimmunity*. 2014;47:419-429.
- Moldovan L, Batte KE, Trgovcich J, Wisler J, Marsh CB, Piper M. Methodological challenges in utilizing miRNAs as circulating biomarkers. *J Cell Mol Med*. 2014;18:371-390.

25. Rice J, Roberts H, Burton J, et al. Assay reproducibility in clinical studies of plasma miRNA. *PLoS One*. 2015;10:1–23.
26. Yin Z, Cui Z, Ren Y, Xia L, Li H, Zhou B. MiR-146a polymorphism correlates with lung cancer risk in Chinese nonsmoking females. *Oncotarget*. 2017;8:2275–2283.
27. Wang S, Liu JC, Ju Y, et al. microRNA-143/145 loss induces Ras signaling to promote aggressive Pten-deficient basal-like breast cancer. *JCI Insight*. 2017;2:e93313.
28. Jabs DA, Nussenblatt RB, Rosenbaum JT. Standardization of uveitis nomenclature for reporting clinical data: results of the First International Workshop. *Am J Ophthalmol*. 2005;140:509–516.
29. Schwochow D, Serieys LEK, Wayne RK, Thalmann O. Efficient recovery of whole blood RNA: a comparison of commercial RNA extraction protocols for high-throughput applications in wildlife species. *BMC Biotechnol*. 2012;12:33.
30. Schwarzenbach H, Da Silva AM, Calin G, Pantel K. Data normalization strategies for microRNA quantification. *Clin Chem*. 2015;61:1333–1342.
31. Livak KJ, Schmittgen TD. Analysis of relative gene expression data using real-time quantitative PCR and the 2(-Delta Delta C(T)) method. *Methods*. 2001;25:402–408.
32. Metsalu T, Vilo J. ClustVis: a web tool for visualizing clustering of multivariate data using Principal Component Analysis and heatmap. *Nucleic Acids Res*. 2015;43:W566–W570.
33. Xia J, Wishart DS. Using MetaboAnalyst 3.0 for comprehensive metabolomics data analysis. In: *Current Protocols in Bioinformatics*. Vol 55. Hoboken, NJ: John Wiley & Sons, Inc.; 2016:14.10.1–14.10.91.
34. Andrés-León E, González Peña D, Gómez-López G, Pisano DG. miRGate: a curated database of human, mouse and rat miRNA-mRNA targets. *Database (Oxford)*. 2015; 2015:bav035.
35. Hamberg M, Backes C, Fehlmann T, et al. MiRTargetLink—miRNAs, genes and interaction networks. *Int J Mol Sci*. 2016; 17:564.
36. Ashburner M, Ball CA, Blake JA, et al; for the Gene Ontology Consortium. Gene ontology: tool for the unification of biology. *Nat Genet*. 2000;25:25–29.
37. Kanehisa M, Goto S. KEGG: Kyoto encyclopedia of genes and genomes. *Nucleic Acids Res*. 2000;28:27–30.
38. Petri V, Jayaraman P, Tutaj J, et al. The pathway ontology - updates and applications. *J Biomed Semantics*. 2014;5:7.
39. Chen J, Bardes EE, Aronow BJ, Jegga AG. ToppGene Suite for gene list enrichment analysis and candidate gene prioritization. *Nucleic Acids Res*. 2009;37(suppl 2):305–311.
40. Rieckmann JC, Geiger R, Hornburg D, et al. Social network architecture of human immune cells unveiled by quantitative proteomics. *Nat Immunol*. 2017;18:583–593.
41. Bruggner RV, Bodenmiller B, Dill DL, Tibshirani RJ, Nolan GP. Automated identification of stratifying signatures in cellular subpopulations. *Proc Natl Acad Sci U S A*. 2014;111:E2770–E2777.
42. Backes C, Sedaghat-Hamedani F, Frese K, et al. Bias in high-throughput analysis of miRNAs and implications for biomarker studies. *Anal Chem*. 2016;88:2088–2095.
43. Mitiushkina NV, Iyevleva AG, Kuligina ES, Togo AV, Miki Y, Imyaninov EN. Biased detection of guanine-rich microRNAs by array profiling: systematic error or biological phenomenon? *J Comput Sci*. 2014;5:351–356.
44. Kuiper JJW, Rothova A, Schellekens PAW, Ossewaarde-van Norel A, Bloem AC, Mutis T. Detection of choroid- and retina-antigen reactive CD8+ and CD4+ T lymphocytes in the vitreous fluid of patients with birdshot chorioretinopathy. *Hum Immunol*. 2014;75:570–577.
45. Chen P, Denniston AK, Hirani S, Hannes S, Nussenblatt RB. Role of dendritic cell subsets in immunity and their contribution to noninfectious uveitis. *Surv Ophthalmol*. 2015;60:242–249.
46. Smith JR, Stempel AJ, Bharadwaj A, Appukuttan B. Involvement of B cells in non-infectious uveitis. *Clin Transl Immunol*. 2016;5:e63.
47. Lipski DA, Dewispelaere R, Foucart V, et al. MHC class II expression and potential antigen-presenting cells in the retina during experimental autoimmune uveitis. *J Neuroinflammation*. 2017;14:136.
48. Moretta L. Dissecting CD56<sup>dim</sup> human NK cells. *Blood*. 2010; 116:3689–3691.
49. Carmona-Rivera C, Kaplan MJ. Low-density granulocytes: a distinct class of neutrophils in systemic autoimmunity. *Semin Immunopathol*. 2013;35:455–463.
50. Geijtenbeek TBH, Gringhuis SI. Signalling through C-type lectin receptors: shaping immune responses. *Nat Rev Immunol*. 2009;9:465–479.
51. Caspi RR. A look at autoimmunity and inflammation in the eye. *J Clin Invest*. 2010;120:3073–3083.
52. Wakefield D, Yates W, Amjadi S, McCluskey P. HLA-B27 anterior uveitis: immunology and immunopathology. *Ocul Immunol Inflamm*. 2016;24:450–459.
53. Mesquida M, Molins B, Llorenç V, de la Maza MS, Adán A. Targeting interleukin-6 in autoimmune uveitis. *Autoimmun Rev*. 2017;16:1079–1089.
54. Zhou Q, Xiao X, Wang C, et al. Decreased microRNA-155 expression in ocular Behcet's disease but not in Vogt-Koyanagi Harada syndrome. *Invest Ophthalmol Vis Sci*. 2012;53:5665–5674.
55. Qi J, Hou S, Zhang Q, et al. A functional variant of pre-miRNA-196a2 confers risk for Behcet's disease but not for Vogt-Koyanagi-Harada syndrome or AAU in ankylosing spondylitis. *Hum Genet*. 2013;132:1395–1404.
56. Yang L, Du L, Yue Y, et al. miRNA copy number variants confer susceptibility to acute anterior uveitis with or without ankylosing spondylitis. *Invest Ophthalmol Vis Sci*. 2017;58: 1991–2001.
57. Adams BD, Parsons C, Walker L, Zhang WC, Slack FJ. Targeting noncoding RNAs in disease. *J Clin Invest*. 2017;127:761–771.
58. Mestdagh P, Hartmann N, Baeriswyl L, et al. Evaluation of quantitative miRNA expression platforms in the microRNA quality control (miRQC) study. *Nat Methods*. 2014;11:809–815.
59. Pasquinelli AE. MicroRNAs and their targets: recognition, regulation and an emerging reciprocal relationship. *Nat Rev Genet*. 2012;13:271–282.
60. Tsang JS, Ebert MS, van Oudenaarden A. Genome-wide dissection of microRNA functions and cotargeting networks using gene set signatures. *Mol Cell*. 2010;38:140–153.
61. Hsu YR, Chang S-W, Lin Y-C, Yang C-H. Expression of MicroRNAs in the eyes of Lewis rats with experimental autoimmune anterior uveitis. *Mediators Inflamm*. 2015; 2015:1–11.
62. Guo D, Li J, Liu Z, Tang K, Song H, Bi H. Characterization of microRNA expression profiling in peripheral blood lymphocytes in rats with experimental autoimmune uveitis. *Inflamm*. 2015;64:683–696.
63. Ifergan I, Chen S, Zhang B, Miller SD. Cutting edge: microRNA-223 regulates myeloid dendritic cell-driven Th17 responses in experimental autoimmune encephalomyelitis. *J Immunol*. 2016;196:1455–1459.
64. Chen P, Urzua CA, Knickelbein JE, et al. Elevated CD1c + myeloid dendritic cell proportions associate with clinical activity and predict disease reactivation in noninfectious uveitis. *Invest Ophthalmol Vis Sci*. 2016;57:1765–1772.
65. Chen P, Tucker W, Hannes S, et al. Levels of blood CD1c+ mDC1 and CD1chi mDC1 subpopulation reflect disease

- activity in noninfectious uveitis. *Invest Ophthalmol Vis Sci.* 2015;56:346-351.
66. Zhou H, Xiao J, Wu N, et al. MicroRNA-223 regulates the differentiation and function of intestinal dendritic cells and macrophages by targeting C/EBP $\beta$ . *Cell Rep.* 2015;13:1149-1160.
  67. Neudecker V, Haneklaus M, Jensen O, et al. Myeloid-derived miR-223 regulates intestinal inflammation via repression of the NLRP3 inflammasome. *J Exp Med.* 2017;214:1737-1752.
  68. Wang H, Chao K, Ng SC, et al. Pro-inflammatory miR-223 mediates the cross-talk between the IL23 pathway and the intestinal barrier in inflammatory bowel disease. *Genome Biol.* 2016;17:58.
  69. Horai R, Sen HN, Caspi RR. Commensal microbiota as a potential trigger of autoimmune uveitis. *Expert Rev Clin Immunol.* 2017;13:291-293.
  70. Aziz F. The emerging role of miR-223 as novel potential diagnostic and therapeutic target for inflammatory disorders. *Cell Immunol.* 2016;303:1-6.
  71. Levinson RD. Killer immunoglobulin-like receptor genes in uveitis. *Ocul Immunol Inflamm.* 2011;19:192-201.
  72. Guan H, Singh UP, Rao R, et al. Inverse correlation of expression of microRNA-140-5p with progression of multiple sclerosis and differentiation of encephalitogenic T helper type 1 cells. *Immunology.* 2016;147:488-498.
  73. Lewkowicz P, Cwiklińska H, Mycko MP, et al. Dysregulated RNA-induced silencing complex (RISC) assembly within CNS corresponds with abnormal miRNA expression during autoimmune demyelination. *J Neurosci.* 2015;35:7521-7537.
  74. Ness T, Boehringer D, Heinzlmann S. Intermediate uveitis: pattern of etiology, complications, treatment and outcome in a tertiary academic center. *Orphanet J Rare Dis.* 2017;12:81.
  75. Olsen TG, Frederiksen J. The association between multiple sclerosis and uveitis. *Surv Ophthalmol.* 2017;62:89-95.
  76. Gordon LK, Goldstein DA. Gender and uveitis in patients with multiple sclerosis. *J Ophthalmol.* 2014;2014:1-5.
  77. Sun J, Tao S, Liu L, Guo D, Xia Z, Huang M. MIR-140-5p regulates angiogenesis following ischemic stroke by targeting VEGFA. *Mol Med Rep.* 2016;13:4499-4505.
  78. Hu Y, Li Y, Wu C, et al. MicroRNA-140-5p inhibits cell proliferation and invasion by regulating VEGFA/MMP2 signaling in glioma. *Tumour Biol.* 2017;39:1-12.
  79. Zhang W, Zou C, Pan L, et al. MicroRNA-140-5p inhibits the progression of colorectal cancer by targeting VEGFA. *Cell Physiol Biochem.* 2015;37:1123-1133.
  80. Xu S, Witmer PD, Lumayag S, Kovacs B, Valle D. MicroRNA (miRNA) transcriptome of mouse retina and identification of a sensory organ-specific miRNA cluster. *J Biol Chem.* 2007;282:25053-25066.
  81. Ertekin S, Yıldırım O, Dinç E, Ayaz L, Fidancı SB, Tamer L. Evaluation of circulating miRNAs in wet age-related macular degeneration. *Mol Vis.* 2014;20:1057-1066.
  82. Momen-Heravi F, Saha B, Kodys K, Catalano D, Satishchandran A, Szabo G. Increased number of circulating exosomes and their microRNA cargos are potential novel biomarkers in alcoholic hepatitis. *J Transl Med.* 2015;13:261.
  83. Savelyeva AV, Kuligina EV, Bariakin DN, et al. Variety of RNAs in peripheral blood cells, plasma, and plasma fractions. *Biomed Res Int.* 2017;2017:1-10.
  84. Mroczek S, Dziembowski A. U6 RNA biogenesis and disease association. *Wiley Interdiscip Rev RNA.* 2013;4:581-592.
  85. Crossland RE, Norden J, Bibby LA, Davis J, Dickinson AM. Evaluation of optimal extracellular vesicle small RNA isolation and qRT-PCR normalisation for serum and urine. *J Immunol Methods.* 2016;429:39-49.
  86. Zheng G, Wang H, Zhang X, et al. Identification and validation of reference genes for qPCR detection of serum microRNAs in colorectal adenocarcinoma patients. *PLoS One.* 2013;8:1-10.
  87. Lim QE, Zhou L, Ho YK, Wan G, Too HP. snoU6 and 5S RNAs are not reliable miRNA reference genes in neuronal differentiation. *Neuroscience.* 2011;199:32-43.
  88. Tang G, Shen X, Lv K, Wu Y, Bi J, Shen Q. Different normalization strategies might cause inconsistent variation in circulating microRNAs in patients with hepatocellular carcinoma. *Med Sci Monit.* 2015;21:617-624.
  89. Xiang M, Zeng Y, Yang R, et al. U6 is not a suitable endogenous control for the quantification of circulating microRNAs. *Biochem Biophys Res Commun.* 2014;454:210-214.
  90. Benz F, Roderburg C, Vargas Cardenas D, et al. U6 is unsuitable for normalization of serum miRNA levels in patients with sepsis or liver fibrosis. *Exp Mol Med.* 2013;45:e42.